

Output Regulation of a Flexible Robot Arm

A. De Luca, L. Lanari, G. Ulivi

Dipartimento di Informatica e Sistemistica
Università degli Studi di Roma "La Sapienza"
Via Eudossiana 18, 00184 Roma, Italy

ABSTRACT

The problem of controlling the motion of a one-link flexible robot arm is considered. A nonlinear dynamic model is derived assuming that the flexibility is represented by elastic springs along the link. Taking as output the end-effector angular position, the resulting zero-dynamics is unstable. Therefore, inversion-based controllers cannot be used for tracking of output trajectories. Instead, it is shown here that a nonlinear regulator approach solves the problem, allowing asymptotic trajectory tracking with internal stability. Simulation results show the good performance of the overall controller and in particular the benefits achieved by a nonlinear design of the regulator.

INTRODUCTION

Trajectory tracking in nonlinear systems has motivated interesting studies [1-3] which have found application in relevant areas like robot motion [4], satellite attitude [5] and induction motor control [6]. Although different terminologies are used for denoting the same control law, exact reproduction of output trajectories is essentially based on feedback controllers which invert the input-output behavior of the plant.

The feasibility of an inversion-based approach relies on the properties of the so-called *zero-dynamics* of the system [7]. In particular, in case of nonlinear systems with no zero-dynamics output tracking is achieved quite easily. Plants that are fully linearizable and decouplable via static or dynamic nonlinear state feedback belong to this class. More in general, the problem of output trajectory tracking can be solved assuming asymptotic stability of the zero-dynamics. Under this hypothesis, the closed-loop system consists of an input-output linear and controllable part, and possibly of an unobservable stable dynamics. From the point of view of system inversion, these nonlinear systems behave like linear ones with no right-half plane zeros, and therefore are usually denoted as minimum phase systems.

On the other hand, direct inversion of *non-minimum phase* nonlinear systems leads to unstable closed-loop behavior. In fact, reproduction of a desired output evolution is attempted in a way equivalent to cancellation of unstable transmission zeros in linear systems. For these cases, control by inversion is not a feasible solution and the tracking problem becomes much more complex.

Robot arms with flexible links under end-effector position control typically display non-minimum phase features [8]. This property is inherited by any realistic finite-dimensional dynamic model of the flexible arm, both in the linear and nonlinear case.

Limitations arising for end-effector tracking in one-link flexible arms have been analyzed in [9,10], together with possible solutions. It is easy to show that assigned joint trajectories can be exactly reproduced in a stable fashion. Extrapolating on this argument, an alternate output point can be defined along the link, and used in place of end-effector position for designing a stable inversion control law. Although satisfactory performance was obtained in terms of tip motion, it is hard to generalize this idea. Moreover, a small but persistent tracking error is present at the end-effector level.

A basically different approach to trajectory tracking has been recently proposed in [11], where the output regulation problem is solved for general nonlinear systems. The underlying idea is that tracking of a prescribed output trajectory can be achieved *without* the need of forcing a linear dynamics in the input-output behavior. Under mild assumptions, a bounded evolution of the state can be associated to a given reference trajectory producing the desired profile at the system output. The regulator is designed so to drive the actual state towards this particular *steady-state* solution, asymptotically obtaining stable output reproduction. As a result, this approach is well suited for facing the output tracking problem in nonlinear non-minimum phase systems.

In this paper, the problem of end-effector motion control for a one-link planar flexible arm is approached in a direct way and solved by means of nonlinear regulation theory. A great effort is expected in order to bring the regulator into action for more complex flexible robotic systems, but the problem considered here, and the particular form of solution proposed, contains most of the aspects which are relevant in the more general case.

In particular, in the robotic application it is useful to combine the regulator approach with an inversion-based control law. The controller design proceeds in two phases: first, a nonlinear inversion feedback is applied to the original plant bringing it to a more convenient canonical form; then, for the compensated system the regulator is set-up and takes care of the possible induced instabilities. A similar control structure has been proposed in [12].

In the following, a nonlinear dynamic model of the flexible arm is introduced. The steps involved in the inversion and in the regulation phases are presented in detail. Numerical simulations are reported illustrating the good performance of a fully nonlinear regulator control design.

MODELING OF A FLEXIBLE ARM

Consider a one-link planar robot with pure bending flexibility. Different finite-dimensional models of flexible arms can be derived but when the analysis is limited to small deflections a linear dynamics is obtained. However, in presence of heavy carried loads and/or in case of fast motion, nonlinear effects arise due to the larger deformations coming into play. For general multi-link flexible arms, the system is governed by equations with even harder nonlinearities, including those due to rigid body motion and couplings of rigid with flexible dynamics. A modeling technique which simply complies with nonlinearities considers the flexible link subdivided into a chain of rigid segments and assumes the deformation concentrated in elastic springs. Multi-link flexible robot arms can be treated in the same way. This representation is similar to the finite-element method, but the model needs not to be limited to small deflections.

With reference to Fig. 1, the Lagrangian dynamics is obtained in the standard form as

$$B(\mathbf{q})\ddot{\mathbf{q}} + \mathbf{c}(\mathbf{q}, \dot{\mathbf{q}}) + \mathbf{e}(\mathbf{q}) + K\mathbf{q} + D\dot{\mathbf{q}} = G\mathbf{u} \tag{1}$$

with $\mathbf{q} \in \mathbb{R}^N$. Explicit expressions parametrized in the number of segments can be given to the terms in (1), so that the model order can be varied easily to achieve the desired accuracy.

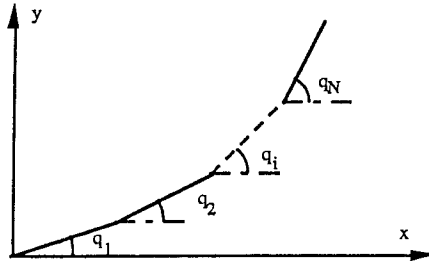


Fig.1 - Discrete modeling of a one-link flexible arm

Taking N equal segments of uniform mass, and denoting by L and M the total link length and mass, the elements of the inertia matrix $B(\mathbf{q})$ are

$$b_{ii} = \frac{ML^2}{N^3} \left(\frac{1}{3} + N - i \right), \quad i = 1, \dots, N,$$

$$b_{ij} = \frac{ML^2}{N^3} \left(\frac{1}{2} + N - \max\{i, j\} \right) \cos(q_i - q_j), \quad i, j = 1, \dots, N.$$

The components of the centrifugal force $\mathbf{c}(\mathbf{q}, \dot{\mathbf{q}})$ are

$$c_i = \sum_{j=1}^n \frac{ML^2}{N^3} \left(\frac{1}{2} + N - \max\{i, j\} \right) \sin(q_i - q_j) \dot{q}_j^2,$$

while those of the gravitational term $\mathbf{e}(\mathbf{q})$ are

$$e_i = \frac{MLg}{N^2} \left(\frac{1}{2} + N - i \right) \cos q_i \cos \gamma,$$

where γ is the angle between the plane of motion and the vertical plane and g is the gravity constant. The linear elasticity matrix K takes on the form

$$K = \begin{bmatrix} k_1 & -k_1 & 0 & \dots & 0 \\ & \ddots & \ddots & \ddots & \\ & -k_{i-1} & k_{i-1} + k_i & -k_i & \\ & & \ddots & \ddots & \ddots \\ 0 & \dots & 0 & -k_{N-1} & k_{N-1} \end{bmatrix},$$

where k_i is the elasticity constant of the i -th spring $i = 1, \dots, N-1$. The viscous damping matrix D has the same structure of K , with the spring damping coefficients d_i 's in place of the k_i 's. A term d_0 should be added in the $(1, 1)$ -element of D , representing the viscous friction at the joint axis. Finally, vector $G = (1 \ 0 \ \dots \ 0)^T$ selects the only equation where

the scalar torque u performs work. The choice of absolute generalized coordinates q results in a more compact model since no Coriolis terms are present. However, it may be convenient to rewrite the system dynamics in terms of relative angles θ_i between segments so to display directly the deflection variables. The transformation between absolute and relative coordinates is a linear one, with $\theta_1 = q_1$ and $\theta_i = q_i - q_{i-1}$, $i = 2, \dots, N$. Note that using variables θ , matrices K and D become diagonal. When the end-effector angular position is chosen as output, a non-minimum phase system is obtained from (1). Moreover, this output has always relative degree 2, independently of the number N of assumed segments [†].

For the sake of clarity, and without loss of generality, the following treatments will be limited to the $N = 2$ case, on a horizontal plane ($\gamma = 90^\circ$). The dynamic equations can be explicitly written as

$$\begin{bmatrix} b_{11}(\theta_2) & b_{12}(\theta_2) \\ b_{12}(\theta_2) & b_{22} \end{bmatrix} \begin{bmatrix} \ddot{\theta}_1 \\ \ddot{\theta}_2 \end{bmatrix} + \begin{bmatrix} c_1(\theta_2, \dot{\theta}_1, \dot{\theta}_2) + d_0 \dot{\theta}_1 \\ c_2(\theta_2, \theta_1) + k_1 \theta_2 + d_1 \dot{\theta}_2 \end{bmatrix} = \begin{bmatrix} 1 \\ 0 \end{bmatrix} u \quad (2)$$

where

$$\begin{aligned} b_{11}(\theta_2) &= a + 2c \cos \theta_2, & b_{12}(\theta_2) &= b + c \cos \theta_2, & b_{22} &= b, \\ c_1(\theta_2, \dot{\theta}_1, \dot{\theta}_2) &= -c(\dot{\theta}_2^2 + 2\dot{\theta}_1 \dot{\theta}_2) \sin \theta_2, & c_2(\theta_2, \theta_1) &= c \dot{\theta}_1^2 \sin \theta_2, \end{aligned}$$

and $a = 5ML^2/24$, $b = ML^2/24$, $c = ML^2/16$. The linearized expression of the end-effector angular position

$$y = \theta_1 + \frac{1}{2}\theta_2 \quad (3)$$

will be taken as controlled output for system (2).

INVERSION-BASED PRECOMPENSATION

The design of an inversion-based controller for output tracking is accomplished deriving twice (3) and setting $\ddot{y} = v$. Solving for the input torque u yields [9]

$$u = c_1(\theta_2, \dot{\theta}_1, \dot{\theta}_2) + d_0 \dot{\theta}_1 + \frac{b_{11}(\theta_2) - 2b_{12}(\theta_2)}{2b_{22} - b_{12}(\theta_2)}(c_2(\theta_2, \theta_1) + k_1 \theta_2 + d_1 \dot{\theta}_2) + \frac{2 \det B(\theta_2)}{2b_{22} - b_{12}(\theta_2)}v, \quad (4)$$

which is in the form of a nonlinear state feedback applied to the flexible arm. After replacing θ_1 with $y - \theta_2/2$, the closed-loop equations become

$$\begin{aligned} \ddot{y} &= v, \\ \ddot{\theta}_2 &= \frac{2(c_2(\theta_2, \dot{\theta}_2, \dot{y}) + k_1 \theta_2 + d_1 \dot{\theta}_2)}{b_{12}(\theta_2) - 2b_{22}} + \frac{2b_{12}(\theta_2)}{b_{12}(\theta_2) - 2b_{22}}v = \alpha(\theta_2, \dot{\theta}_2, \dot{y}) + \beta(\theta_2)v. \end{aligned} \quad (5)$$

To track a desired output trajectory $y_d(t)$, the linear input-output behavior in (5) is stabilized by

$$v = \ddot{y}_d + k_D(\dot{y}_d - \dot{y}) + k_P(y_d - y), \quad (6)$$

[†] This is true in a generic sense, i.e. except for a unique combination of arm mechanical parameters [9].

but the critical issue here is the instability of the unobservable closed-loop dynamics. As a matter of fact, the associated zero-dynamics obtained with $y \equiv 0$

$$\ddot{\theta}_2 = -\frac{(c/2)\dot{\theta}_2^2 \sin \theta_2 + 2(k_1 \theta_2 + d_1 \dot{\theta}_2)}{b - c \cos \theta_2} \quad (7)$$

turns out to be unstable. Therefore, the inversion-based controller (4)–(6) cannot be used as such for output reproduction, and this situation calls for a nonlinear regulator approach. However, there is still a benefit in using (4) as a precompensation on the original plant. The resulting intermediate system (5) is in fact already in a nice canonical form, with the main nonlinearities removed by feedback from the input-output path. The design of a regulator will take advantage of this internal structure.

NONLINEAR REGULATOR DESIGN

The instability of the unobservable states in (5) requires counteractions to be taken with the new control input v , other than just stabilization of the input-output behavior. Instead, v will be designed so to attract the state trajectory to a particular *steady-state* manifold, which depends on the reference trajectory. State evolution on this surface, which will be invariant for the closed-loop system, produces as output the desired trajectory. Thus, if the initial state lies on the manifold output tracking will be exact. Otherwise, the output will not follow the desired one during a transient phase until the state has (exponentially) converged to the manifold, so that asymptotic tracking is obtained.

The necessary and sufficient conditions found in [11] for solving the regulation problem in nonlinear systems are recalled. Consider a system given by

$$\dot{\mathbf{x}} = f(\mathbf{x}) + g(\mathbf{x})\mathbf{u}, \quad \mathbf{y} = h(\mathbf{x}), \quad (8)$$

and assume that its linear approximation at $\mathbf{x} = \mathbf{0}$ is stabilizable by means of a linear feedback $\mathbf{u} = F\mathbf{x}$. A reference trajectory $\mathbf{y}_R(t)$ is supposed to be generated by an autonomous dynamic system (i.e. the exosystem)

$$\dot{\mathbf{w}} = s(\mathbf{w}), \quad \mathbf{y}_R = q(\mathbf{w}), \quad (9)$$

for which every point in an open neighborhood of the stable equilibrium $\mathbf{w} = \mathbf{0}$ is Poisson stable (see [7], p.352). Vector functions f and h are assumed to be zero at $\mathbf{x} = \mathbf{0}$, as well as s and q at $\mathbf{w} = \mathbf{0}$. Define two mappings $\mathbf{u} = c(\mathbf{w})$ and $\mathbf{x} = \pi(\mathbf{w})$ being at least C^2 , with $c(\mathbf{0}) = \mathbf{0}$ and $\pi(\mathbf{0}) = \mathbf{0}$. A state feedback of the form

$$\mathbf{u} = c(\mathbf{w}) + F(\mathbf{x} - \pi(\mathbf{w})) \quad (10)$$

solves the Regulator Problem [11] if and only if $c(\mathbf{w})$ and $\pi(\mathbf{w})$ satisfy the following equations

$$\begin{aligned} \frac{\partial \pi}{\partial \mathbf{w}} s(\mathbf{w}) &= f(\pi(\mathbf{w})) + g(\pi(\mathbf{w}))c(\mathbf{w}), \\ q(\mathbf{w}) &= h(\pi(\mathbf{w})). \end{aligned} \quad (11)$$

The resulting nonlinear regulator (10) is made of a feedforward term $c(\mathbf{w})$, providing the desired steady-state response, plus a feedback designed around the surface $\mathbf{x} = \pi(\mathbf{w})$, which is a manifold in the extended state space.

This control approach will be applied next to the flexible arm, assuming the inversion feedback law (4) has already been used for precompensation. The system state is $\mathbf{x} = (y, \dot{y}, \theta_2, \dot{\theta}_2)$. Stabilizability of the linear approximation of (5) (or equivalently of (2)) is easily verified. Consider as reference trajectory a sinusoidal function $y_R(t) = A \sin(\omega t + \phi)$, which can be generated by a properly initialized second-order exosystem

$$\dot{\mathbf{w}} = \begin{bmatrix} \dot{w}_1 \\ \dot{w}_2 \end{bmatrix} = \begin{bmatrix} \omega w_2 \\ -\omega w_1 \end{bmatrix} = s(\mathbf{w}), \quad y_R = w_1 = q(\mathbf{w}). \quad (12)$$

Equations (11) become in this case

$$\begin{aligned} \frac{\partial \pi_1}{\partial w_1} \omega w_2 - \frac{\partial \pi_1}{\partial w_2} \omega w_1 &= \pi_2(\mathbf{w}), & \frac{\partial \pi_2}{\partial w_1} \omega w_2 - \frac{\partial \pi_2}{\partial w_2} \omega w_1 &= c(\mathbf{w}), \\ \frac{\partial \pi_3}{\partial w_1} \omega w_2 - \frac{\partial \pi_3}{\partial w_2} \omega w_1 &= \pi_4(\mathbf{w}), & \frac{\partial \pi_4}{\partial w_1} \omega w_2 - \frac{\partial \pi_4}{\partial w_2} \omega w_1 &= \alpha(\pi(\mathbf{w})) + \beta(\pi(\mathbf{w}))c(\mathbf{w}), \\ w_1 &= \pi_1(\mathbf{w}), \end{aligned} \quad (13)$$

with α and β defined in (5). Exploiting the particular form of these partial differential equations, it is straightforward to see that

$$\pi_1(\mathbf{w}) = w_1, \quad \pi_2(\mathbf{w}) = \omega w_2, \quad c(\mathbf{w}) = -\omega^2 w_1. \quad (14)$$

Note that the feedforward term $c(\mathbf{w})$ is just the desired output acceleration. By using (14), system (13) is reduced to the last two P.D.E. which are the first-order counterpart of the unobservable dynamics in (5). Therefore, once $\pi_3(\mathbf{w})$ is determined analytically, $\pi_4(\mathbf{w})$ can be obtained by explicit time derivation. Since a closed-form solution is hard to find, standard methods of approximation can be used, e.g. by polynomial expansions. In particular, assuming for π_3 a complete polynomial of third degree

$$\pi_3 \approx a_1 w_1 + a_2 w_2 + a_{11} w_1^2 + a_{12} w_1 w_2 + a_{22} w_2^2 + a_{111} w_1^3 + a_{112} w_1^2 w_2 + a_{122} w_1 w_2^2 + a_{222} w_2^3, \quad (15)$$

a solution has been computed substituting (15) into (13), expanding in Mac Laurin series the nonlinear functions $\alpha(\mathbf{w})$ and $\beta(\mathbf{w})$, and retaining terms up to the third order. Simple calculations show that the coefficients a_{11} , a_{12} , and a_{22} are zero in the solution. The regulation control law is then fully determined as

$$v = c(w_1) + \sum_{i=1}^4 F_i(x_i - \pi_i(w_1, w_2)). \quad (16)$$

It should be stressed that the actual input torque u to the arm is the composition of (16) and (4). A block diagram of the overall controller is reported in Fig. 2.

As an useful comparison, a linearized version of the regulator (16) can be obtained within the present framework, by simply limiting the above expansions to first order

terms. Equivalently, a standard regulator may be designed on the linear approximation of system (5). Note however that this does not yield a fully linear regulator for the original model (2), because the inversion-based nonlinear precompensation is still present.

SIMULATION RESULTS

The nonlinear regulator for the one-link flexible arm has been tested on two types of end-effector output trajectories, a continuous sinusoidal motion and a point-to-point task with a half-wave sinusoidal velocity profile. The mechanical parameters of the flexible arm are $L = 1$ m, $M = 0.2$ kg, $k_1 = 5$ Nm/rad, $d_0 = d_1 = 0.01$ Nm sec/rad. The simulations were run using a third order Runge-Kutta method with adaptive integration step.

For the sinusoidal motion, an amplitude $A = 0.05$ rad, an angular frequency $\omega = 20\pi$ rad/sec and a phase-shift $\phi = \pi/2$ were selected as exosystem parameters. Note that the chosen signal frequency is well beyond the natural resonance of the arm. The arm starts from the undeformed rest position with an initial tip error of 0.1 rad. The linear feedback matrix F is selected so to place the poles of the linear part of the closed-loop system at $[-20, -20, -30, -30]$. The obtained tip angular motion is reported in Fig. 3, together with the desired one which is perfectly reproduced after about four periods. Fig. 4 shows that the input torque applied to the arm has a very smooth behavior even during the transient phase. Moreover, the system nonlinearities are clearly displayed by the non-sinusoidal behavior at steady-state. The deflection amplitude θ_2 , representing the unobservable part of the closed-loop system, and the joint position θ_1 are reported in Fig. 5; as expected, θ_2 remains limited. Note also that tip as well as joint motions are in opposite phase with the flexible variable. For comparison purposes, Figs. 6 and 7 report the output error, i.e. the difference between actual and desired output, obtained with nonlinear regulation or, respectively, with the linear approximation discussed in the previous section. Although the two waveforms look similar, the second one shows a residual error even at steady-state, because of neglected nonlinearities.

As a typical robotic trajectory task, a point-to-point tip motion of 90° in one second has been considered next and the results with nonlinear regulation are shown in Figs. 8-11. The trajectory tracking performance is very good. The regulation torque is compared in Fig. 9 with the one computed for an equivalent rigid arm ($k_1 = \infty$), giving evidence of the reduced effort needed during the travel in the flexible case. Joint and tip velocity, reported in Fig. 10, differ only during the transients due to unmatched initial conditions. In fact, even if this significant reference trajectory can be generated by a sinusoidal exosystem, the starting and stopping processes act as abrupt changes in the angular frequency ω or as reset operations of the exosystem internal state. Some transient error will then arise even if the states on the input-output path are matched with the desired trajectory and the corresponding derivatives. This condition is not sufficient to keep the output error at zero. Such a behavior is illustrated in Fig. 11.

CONCLUSIONS

The problem of tracking a desired end-effector trajectory for a flexible robot arm is conveniently solved in two steps. First an inversion-based feedback control is used as a

precompensation on the original system, then the design of the controller is completed by means of the nonlinear regulator approach. Of course, one may use the nonlinear regulator approach directly on the original plant. Changes result in the transient behavior but not at steady-state. The overall feedforward/feedback approach is a viable design tool which avoids hand-crafted solutions, but still retains space for intuition. For robotic applications, the need of an exosystem for defining reference trajectories may be somewhat limiting. For example a slowly-varying sinusoidal profile and a ramp (unbounded) reference can be asymptotically tracked but are generated by exosystems which are not in the theoretical frame worked out until now.

REFERENCES

- [1] R.M. Hirschorn, "Invertibility for multivariable nonlinear control systems", *IEEE Trans. Automatic Control*, vol. AC-24, no. 6, pp. 855-865, 1979.
- [2] R.M. Hirschorn, "Output tracking in multivariable nonlinear systems", *IEEE Trans. Automatic Control*, vol. AC-26, no. 2, pp. 593-595, 1981.
- [3] S.N. Singh, "Generalized functional reproducibility condition for nonlinear systems", *IEEE Trans. Automatic Control*, vol. AC-27, no. 4, pp. 958-960, 1982.
- [4] T.J. Tarn, A.K. Bejczy, A. Isidori, and Y. Chen, "Nonlinear feedback in robot arm control", in *Proc. 23rd Conf. on Decision and Control* (Las Vegas, NV, Dec. 12-14, 1984), pp. 736-751.
- [5] T.A.W. Dwyer III, "Exact nonlinear control of large angle rotational maneuvers", *IEEE Trans. Automatic Control*, vol. AC-29, no. 9, pp. 769-774, 1984.
- [6] A. De Luca and G. Ulivi, "Design of an exact nonlinear controller for induction motors", *IEEE Trans. Automatic Control*, vol. AC-34, no. 12, 1989.
- [7] A. Isidori, *Nonlinear Control Systems*, 2nd Edition, Springer Verlag, Berlin, 1989.
- [8] R.H. Cannon, Jr. and E. Schmitz, "Initial experiments on the end-point control of a flexible one-link robot", *Int. J. Robotics Res.*, vol. 3, no. 3, pp. 62-75, 1984.
- [9] A. De Luca, P. Lucibello, and G. Ulivi, "Inversion techniques for trajectory control of flexible robot arms", *J. Robotic Syst.*, vol. 6, no. 4, pp. 325-344, 1989.
- [10] A. De Luca and B. Siciliano, "Trajectory control of a nonlinear one-link flexible arm", *Int. J. Contr.*, vol. 50, no. 5, pp. 1699-1715, 1989.
- [11] A. Isidori and C. Byrnes, "Output regulation of nonlinear systems", *IEEE Trans. Automatic Control*, vol. AC-35, no. 2, 1990 (To appear).
- [12] P. Lucibello, "Nonlinear regulation, with internal stability, of a two link flexible robot arm", in *Proc. 28th Conf. on Decision and Control* (Tampa, FL, Dec. 13-15, 1989), pp. 1645-1650.

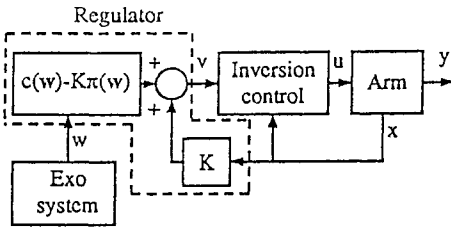


Fig.2 - Control system block diagram

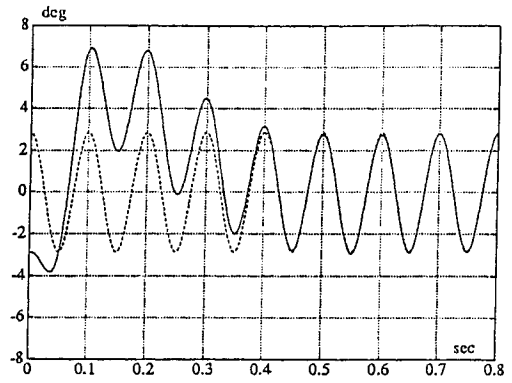


Fig.3 - Output tracking of a cosine wave

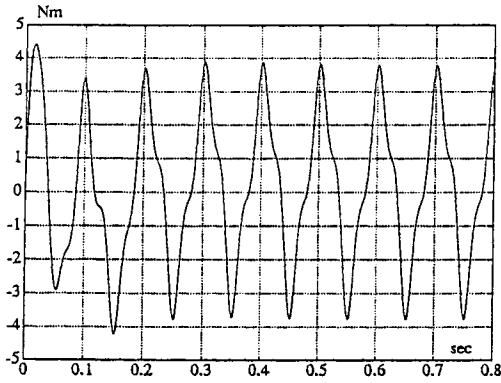


Fig.4 - Motor torque

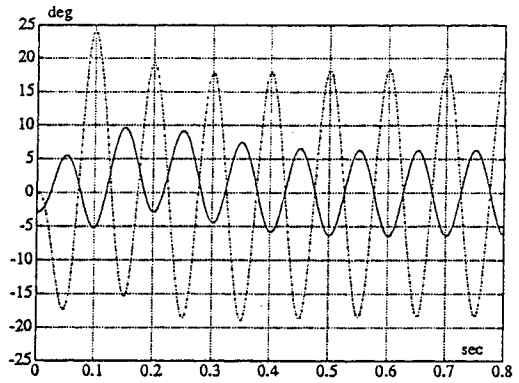


Fig.5 - Joint (-) and flexible (....) variable

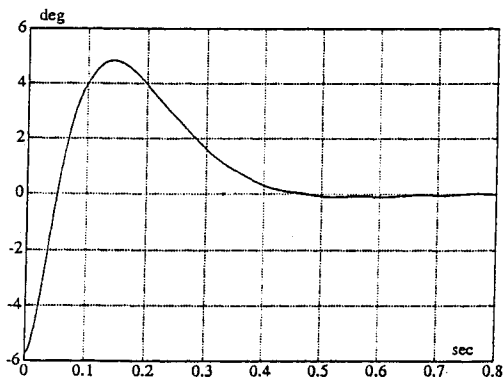


Fig.6 - Output error with nonlinear regulator

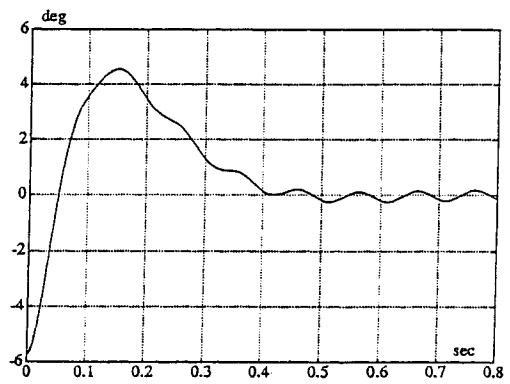


Fig.7 - Output error with approximate regulator

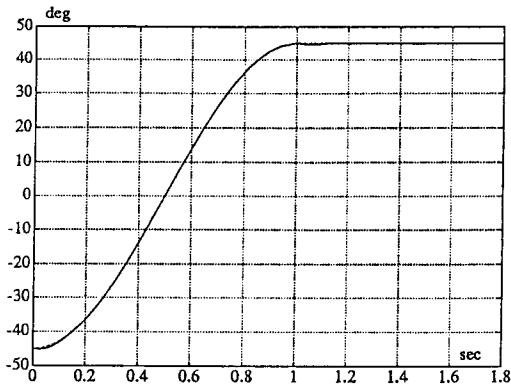


Fig.8 - Output tracking of a point-to-point trajectory

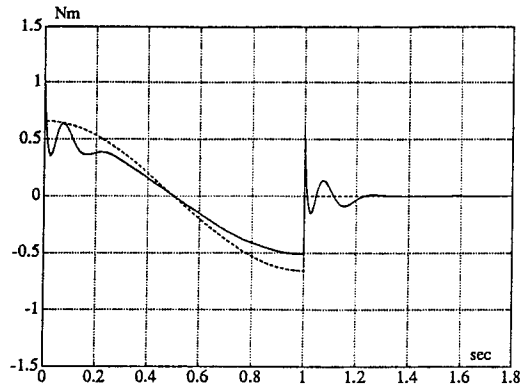


Fig.9 - Motor torque (-- = rigid equivalent)

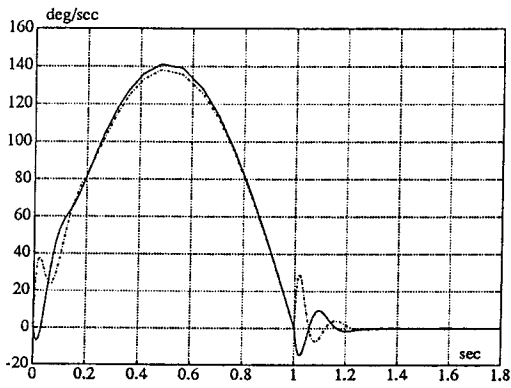


Fig.10 - Joint (....) and tip (-) velocity

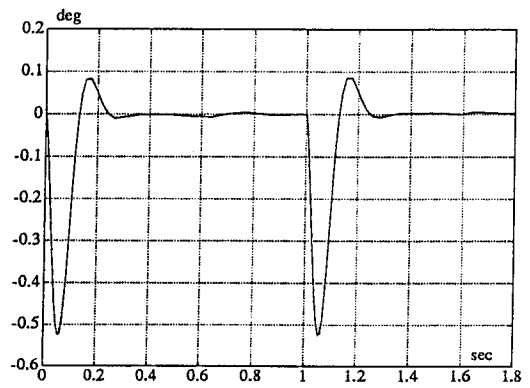


Fig.11 - Output error